Erosion Wear Behavior of Bamboo Fiber-Reinforced High-Density Polyethylene Composites with Nano Silicon Dioxide Filler Subjected to Rotary Water Jet

Xiaokai Li,[a] Jingjing Fu,[b,]* and Liangpeng Jiang [a,]*

The erosion wear behavior of bamboo fiber-reinforced high-density polyethylene (HDPE) composites with silicon dioxide (SiO_2) nanoparticles filler was investigated based on the sand-carrying water (a mixture of water and garnet sand) jets (SCWJ). The composites consisted of varying weight percentage of SiO_2 fillers were prepared through press molding technology. Based on the rotating water jet technique, the erosion wear performance of composites was considered with varying erosion times and shooting distances. The results showed that composites filled with SiO_2 possessed better resistance to SCWJ erosion. The erosion resistance of the composites highly corresponds to their impact strength. The maximum erosion rate occurred at a shooting distance of 0.5 cm and an erosion duration of 180 s. Scanning electron microscopy (SEM) and energy-dispersive spectroscopy (EDS) analysis further demonstrated that the erosive wear mechanisms mainly included the pulverization of bamboo fibers, brittle fracture of HDPE matrix, and increase in oxygen content.

DOI: 10.15376/biores.17.3.5178-5189

Keywords: Silicon dioxide; Bamboo flour; High-density polyethylene; Composites; Rotating waterjet; Erosion wear

Contact information: a: School of Mechanical Engineering, Anhui University of Science and Technology, Huainan 232001, China; b: Nanjing Institute of Agricultural Mechanization, Ministry of Agriculture and Rural Affairs, Nanjing 210014, China;
** Corresponding authors: tutujing12@163.com, jianglp98@outlook.com*

INTRODUCTION

Wood-plastic composites (WPC) are green composites prepared with plant fibers as the filler phase and thermoplastics as the matrix phase. They are widely used in coastal engineering infrastructure, such as ports, docks, and waterways (Xue 2016). However, the current application of WPC in the coastal environment still has certain shortcomings, such as poor hydrodynamic erosion wear resistance and unsatisfactory water resistance. The research on the mechanical (Zhang 2014; Zhang *et al.* 2016), thermal (Fang *et al.* 2013; Guo *et al.* 2014), aging (Zhang *et al.* 2013; Wang *et al.* 2019), and degradation (Moreno *et al.* 2018; Jiang *et al.* 2019) properties of WPC has received extensive attention, but little research has been reported on their hydrodynamic erosion wear properties.

The classifications of wear of WPC under actual working conditions are sliding wear (Jiang *et al.* 2017), abrasive wear (Jeamtrakull *et al.* 2012), and erosion wear (Chand *et al.* 2007; Gupta *et al.* 2012; Bagci and Imrek 2016; Gupta 2018a). Hydrodynamic erosion wear is a common wear form in the field of coastal engineering. It can be described as a type of wear phenomenon in which the material surface is damaged by the impact of a fluid containing solid particles. Jena *et al.* (2018) and Vigneshwaran *et al.* (2019) found that red mud and hollow microbeads could enhance the erosion wear resistance of bamboo fiber-reinforced polymer (BFRP) composites based on an air jet technique, which due to red mud and hollow microbeads with brittle characteristics could develop semi-ductile property of composites. And they pointed out that the erosion speed was the most important parameter affecting the erosion wear. Gupta *et al.* (2012) and Gupta (2018b) have studied the erosive wear properties of BFRP composites using the air jet technique. They found that alumina trioxide and silicon carbide could exhibit ductile behavior when impacted with fine particles, and further improve the erosion wear resistance of BFRP composites, and the highest erosion rate of pneumatic abrasives on BFRP composites was formed at an erosion angle of 75°. The erosion wear mechanism was mainly fiber thinning, fiber crushing and matrix brittle fracture. Most researchers have studied the effect of inorganic particles on the abrasive wear resistance of composites, and there are few reports on the hydraulic wear resistance of composites, with even fewer reports combining the actual working conditions of the materials.

Nano silicon dioxide (SiO_2) is often used as a filler modifier for WPC due to its large specific area and high surface energy. The mechanical properties of SiO_2-filled polymer composites have been studied, while there is no research on their resistance to hydrodynamic erosion wear. Therefore, in view of the wide application of WPC in coastal engineering, the rotating water jet technology is adopted in this paper, which can better simulate the real erosion characteristics of seawater. The effect of SiO_2 on the erosion wear behavior of WPC was investigated to provide a theoretical basis and technical reference for the preparation of erosion-resistant WPC and broaden their application in coastal engineering.

EXPERIMENTAL

Materials

Bamboo fiber (149 μm, yellowish-brown powder, chemical compositions: cellulose 48.78 wt%, hemicellulose 18.21 wt%, lignin 15.60 wt%, ash 3.53 wt%; mechanical milling) was provided by Mujiang Weihua Perfumery Plant, Jiangmen, China. High-density polyethylene (HDPE, 0.85mm, white powder, density: 0. 0.94-0.96 g·cm^{-3}) was obtained from Sinopec Group Co., Ltd., Beijing, China. Maleic anhydride grafted polyethylene (MAPE, white power, density: 0.951 g·cm^{-3}) was acquired from Jinghong Polymer Materials Co., Ltd., Guangdong, China. Silicon dioxide (SiO_2, 20 nm, whiter power) purchased from Keze Metal Materials Co, Ltd, Hebei, China. Garnet sand was purchased from Wuxi Dinglong Mining Co, Ltd. Jiangsu, China.

Table 1. Designation and Composition of Composite Samples

Sample ID	Mass ratio (wt%)			
	SiO_2	Bamboo flour	HDPE	MAPE
S1	0	80	100	3
S2	2	80	100	3
S3	4	80	100	3
S4	6	80	100	3
S5	8	80	100	3

Composite Fabrication

Bamboo powder, HDPE, MAPE, and SiO_2 were dried at 100 °C for 6 h before preparation. The dried raw materials were evenly mixed in the ball grinder (YL71-4, Zhejiang Donglai Motor Co., Ltd.; ceramic ball with 1 cm diameter) with reference to the sample composition ratios in Table 1. The mixed raw materials were molded by XW-212C flat vulcanizing machine (Dongguan Xunwei Testing Instruments Co., Ltd, Guangdong, China) with the molding temperature, pressure and time of 170 °C, 30 MPa, and 12 min, respectively. The specimen size was 100 × 100 × 5 mm^3, and then the sample was cut according to the required size for characterization.

Characterization

The hardness of the samples was tested using the LX-D-1 shore durometer (Siwei Instrument Manufacturing Co., Ltd, Shanghai, China) with an indenter pressure of 0 to 45 N according to GB/T 2411 (2008). The measurements were represented by at least five replications.

The impact strength test of the specimens was carried out by the FBS-5.5DZ pendulum impact tester (Furbs Testing Equipment Co., Ltd., Xiamen, China) according to ASTM D256-10 (2018). The test was conducted at a pendulum impact energy of 2.75 J and an impact velocity of 3.4 m/s. The size of each sample is 100 × 10 × 50 mm^3. Each impact strength value is the mean of at least five specimens.

The water absorption of the samples was tested using the FA224 electronic analytical balance (Furbs Testing Equipment Co., Ltd., Xiamen, China) referring to GB/T 1034 (2008). The samples were dried at 100 °C for 6 h before testing, and then soaked in deionized water at 23 ± 1 °C. The water absorption rate (WA) was calculated from the weight gains according to the following formula:

$$WA=(WA_2-WA_1)/WA_1\times 100\% \tag{1}$$

where WA_1 and WA_2 are the weight of the dry and wet samples (g), respectively.

Microscopic morphology and element investigation were identified by the FlexSEM1000 scanning electron microscopy (SEM, IXRF Ltd., Austin, USA) equipped with 550i energy dispersive spectroscopy (EDS). The location of the surface for the observation was the impact section, the uneroded and eroded surfaces of the sample. The detected surfaces were sputter-coated with gold-palladium to provided electrical conductivity.

The self-assembled former mixed abrasive water jet device (Fig. 1) was used for the erosion wear test. The working principle is that the water is first pumped using a high-pressure reciprocating piston pump into the abrasive tank through the mix chamber until the abrasive tank is filled. Then the sand valve is opened, allowing the water and garnet sand to be mixed in the mix chamber and simultaneously transformed into a rotating jet by a rotating impeller and ejected by a nozzle with an inner diameter of 4 mm. The ejected mixture is called sand-carrying water jets, which is abbreviated as SCWJ. Here, the garnet sand was used as a solid particle carried by the rotating jet, which is more responsive to the state of real seawater. Test was conducted with two control factors: shooting distance (0.5 cm, 1 cm, 1.5 cm) and erosion duration (60 s, 120 s, 180 s). Detailed information about the erosion wear test is shown in Table 2. The shoot distance is the distance between nozzle and sample. The position of nozzle can be adjusted by numerical control platform. Before and after the test, the specimens were subjected to ultrasonic cleansed at 40 kHz for 5 min and dried at 100 °C for 6 h. The loss of erosion weight and the density of samples were measured using an FA224 electronic analytical balance and DM-300 electronic densitometer (Furbs Testing Equipment Co., Ltd., Xiamen, China), respectively. The results were the average of minimum five replicates.

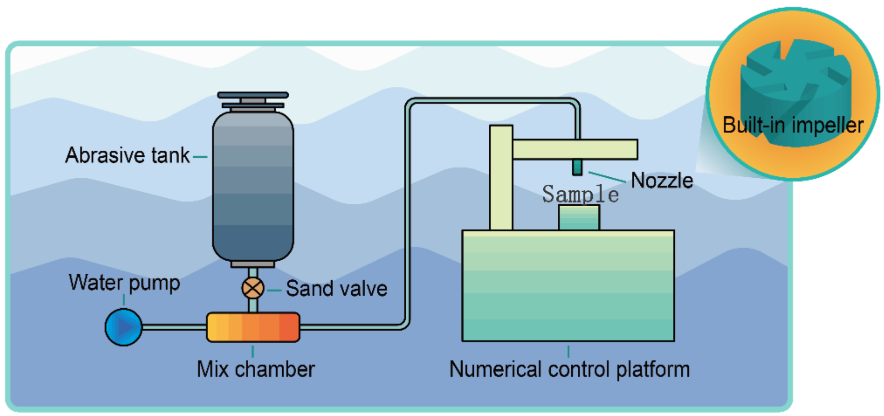

Fig. 1. Schematic diagram of the former mixed abrasive water jet device

Table 2. Detailed Information about the Erosion Wear Test

Erosion Angle	Pump Pressure	Garnet Sand Content	Garnet Sand Size	Specimen Dimensions
90°	1 MPa	0.27 wt%	80 mesh	50 × 50 × 5 mm^3

RESULTS AND DISCUSSION

Erosive Wear Quantification Analysis

The weight and volume losses of bamboo powder-HDPE composites are shown in Fig. 2. Under the same erosion duration, the weight and volume losses of all five samples generally tended to decrease with the increasing shooting distance, which can be explained by the weakening of the SCWJ energy caused by the increase in the shooting distance. However, the weight and volume losses of all samples showed the expected increasing trend with increasing erosion time under the same shooting distance condition. The maximum erosion rate occurred at the shooting distance of 0.5 cm and the erosion duration of 180 s. The maximum weight losses of samples S1, S2, S3, S4, and S5 were 29.6, 21, 18.2, 26, and 27 mg, respectively, and the maximum volume losses were 43, 32.1, 27.6, 38, and 40 mm^3, respectively. It can also be concluded from Fig. 2 that the erosion resistance samples followed the order: S3>S2>S4>S5>S1, indicating that SiO_2 can improve the erosion resistance of bamboo powder-HDPE composites. The effect of SiO_2 addition on the erosion resistance will be further analyzed and verified combined with the analysis of the mechanical properties, micro-morphology and chemical structure of bamboo powder-HDPE composites.

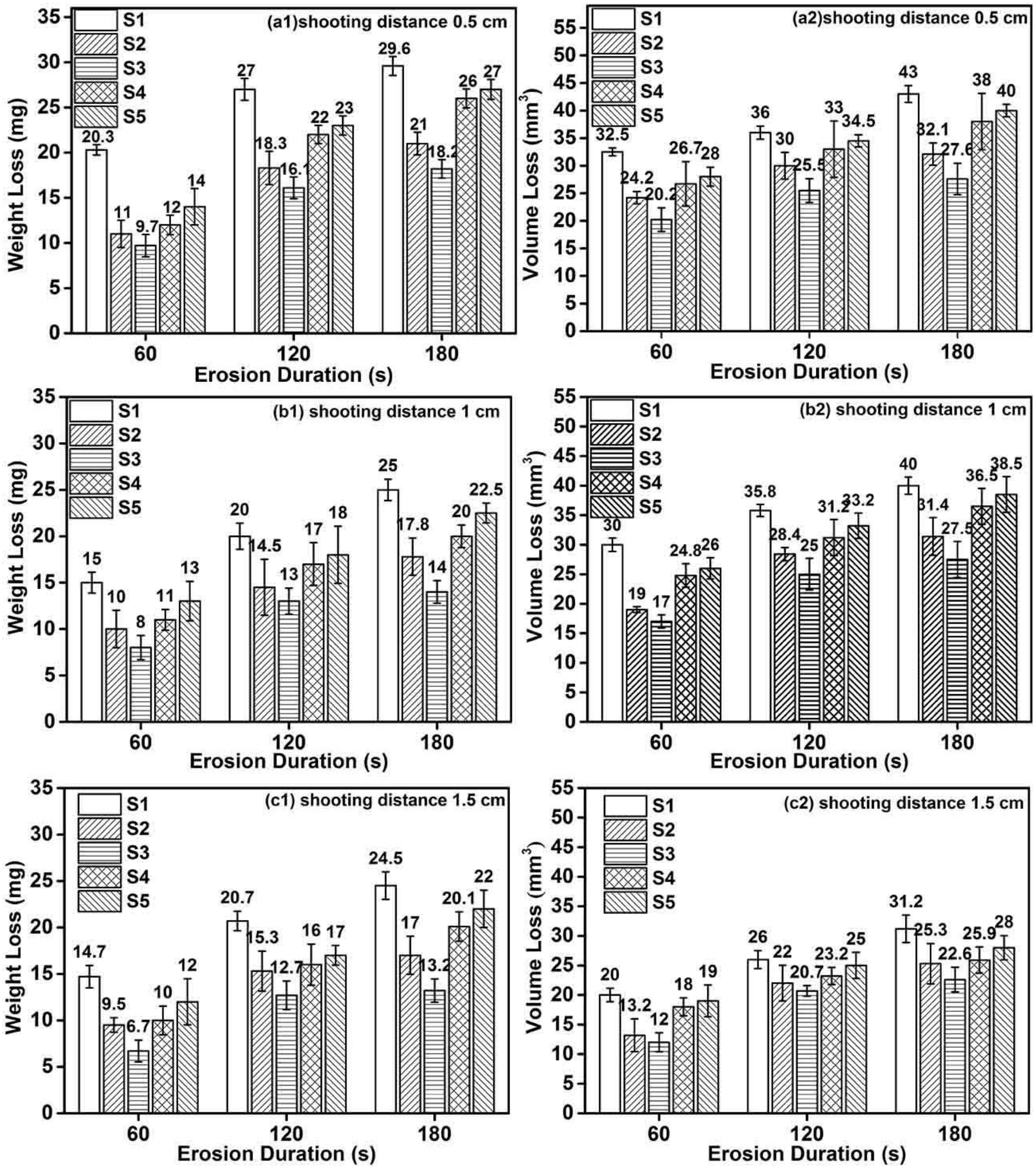

Fig. 2. Weight and volume loss of bamboo powder-HDPE composites

Analysis of Composite Structure

The fiber/matrix interface quality is the key to determine the structural strength and wear properties of WPC (Rashid *et al.* 2017; Swain and Biswas 2017). Therefore, the water absorption (WA) test and impact section microscopy were adopted to laterally characterize the effect of SiO_2 on the fiber/matrix interfacial quality of composites.

The WA test results of the specimens are presented in Fig. 3. As shown in Fig. 3(a), with the increase of soaking time, the dynamic WA of composites showed an upward trend of first fast and then slow until saturation, which is consistent with Fick's law. It is generally believed that a better fiber/matrix interface leads to more comprehensive encapsulation of the hydrophilic fibers by the hydrophobic matrix. All SiO_2-added composites showed lower dynamic WA in comparison with the sample without SiO_2 (S1), which illustrated that SiO_2 could enhance the compatibility of the fiber/matrix interface. From the results of saturated WA (Fig. 3b), compared with the of sample S1 (8.08%), the decrease of saturated water absorption of specimens S2, S3, S4, and S5 were 15.1%, 16.3%, 14.4%, and 14.0%, respectively. It can be concluded from the WA test that sample S3 possessed the best fiber/matrix interface quality, followed by S2, S4, S5, and S1.

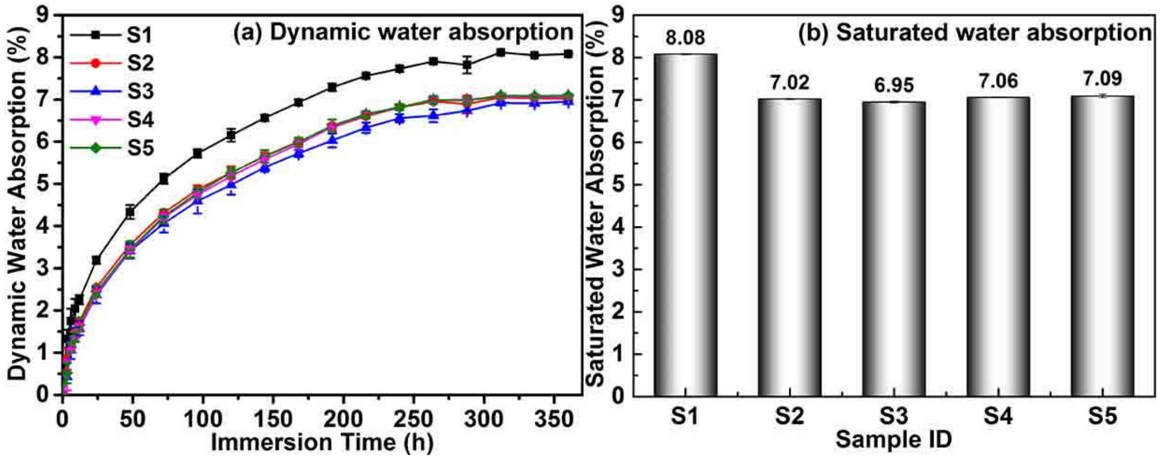

Fig. 3. Dynamic and saturated water absorption of bamboo powder-HDPE composites

The microscopic morphology of the impact cross-section of the bamboo powder-HDPE composite is displayed in Fig. 4. The cross section of sample S1 was uneven and ravine-shaped, and there were strip-shaped void defects left caused by a large number of pulled-out bamboo fibers. The fiber/matrix interface was clearly visible (Fig. 4a). In the impact cross section of sample S2 and S3 (Fig. 4b, 4c), the bamboo fibers were evenly distributed in the HDPE matrix and well wrapped by the HDPE matrix.

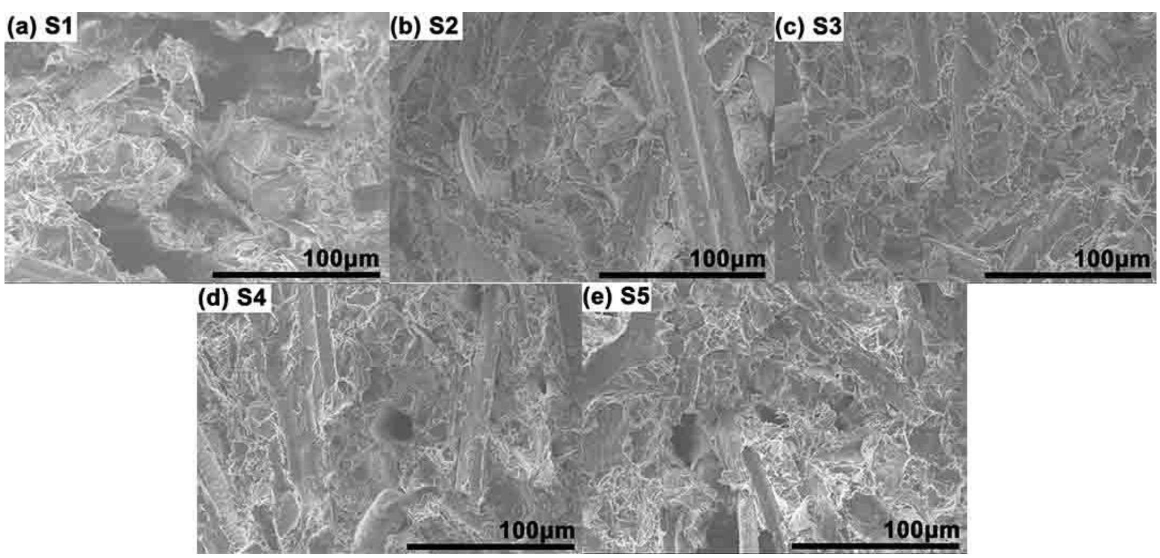

Fig. 4. Impact cross section micromorphology of bamboo powder-HDPE composites

Two phases were tightly bonded and the cross section was flat. For the samples S4 and S5 (Fig. 4d, 4f), the fiber/matrix inter-face was blurred, but there were still a few holes formed by the bamboo fibers being pulled out from the matrix. The microscopic observation of the impact cross section could better confirm the conclusion drawn from the water absorption test. The fiber/matrix inter-face of the samples gradually became indistinct with increasing SiO_2 content, but when the SiO_2 content was too high, a small number of pull-out hole defects appeared at the fiber/matrix interface.

Hardness and Impact Strength Analysis

The erosion rate as well as the type, hardness, and impact strength of the eroded specimens are important experimental parameters affecting the erosion wear properties of the composites (Tilly 1969; Tewari *et al.* 2003). Hence, it is crucial to investigate the synergistic effects of hardness and impact strength on the erosion wear properties of composites.

The hardness and impact strength of composites are given in Fig. 5. The hardness and impact strength of samples showed a trend of first increasing and then decreasing with the increase of SiO_2 content. The hardness of S4 was the highest about 64.6 HD, which increased by 5.6% compared with S1. The impact strength of S3 was the highest about 3.6 KJ m^{-2}, which increased by 11.8% compared with S1. According to the analysis, the increase in hardness and impact strength is due to the large specific surface area and high specific surface energy of nanoscale SiO_2, which can be physically cross-linked with the macromolecular chains of HDPE matrix and tightly bonded. When the HDPE matrix was subjected to the external forces, the physical cross-linking point formed by nanoscale SiO_2 and HDPE can inhibit the sliding of the molecular chains of the matrix (Asgari *et al.* 2017). The decrease in hardness and impact strength is due to the agglomeration of excessively high content of SiO_2, the agglomerated SiO_2 tended to accumulate stress and further causing stress damage.

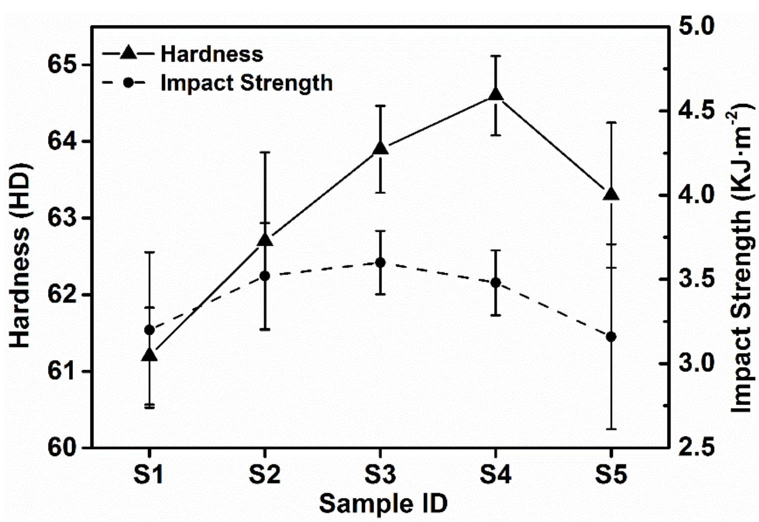

Fig. 5. Hardness and impact strength of bamboo powder-HDPE composites

The erosive wear quantification analysis showed that the sample S3 possessed the best erosion resistance. Combined with the results of composite structure and mechanical properties of bamboo powder-HDPE composites, a reliable explanation for S3 is that it has the relatively best impact strength and fiber/matrix interface, with a hardness second only to that of S4. The higher impact strength provides a stronger resistance to axial SCWJ impact. The better fiber/matrix interface enhances the "anchoring" effect of the matrix on the bamboo fibers and hence improves the interaction force between the matrix and the fibers. The higher hardness provides a stronger resistance to embedding and plowing. However, the larger weight loss of the samples S4 and S5 might because the agglomerated SiO_2 is easily deprived under the action of the SCWJ.

Erosive Wear Mechanism Analysis

The trajectory of the fluid plasmas in the rotating water jet is similar to a conical spiral, and each fluid plasmas has three partial velocities, *i.e.*, axial velocity (*u*), radial velocity (*v*), and tangential velocity (*w*), as shown in Fig. 6. The traditional straight water jet erosion wear technique lacks the tangential velocity. Therefore, compared with the traditional straight water jet, the rotating water jet can reflect the real erosion characteristics of seawater more comprehensively. At the same time, in comparison with direct jet erosion, the erosion wear mechanism of rotary jet is more complex, which requires in-depth analysis based on the characteristics of rotary jet.

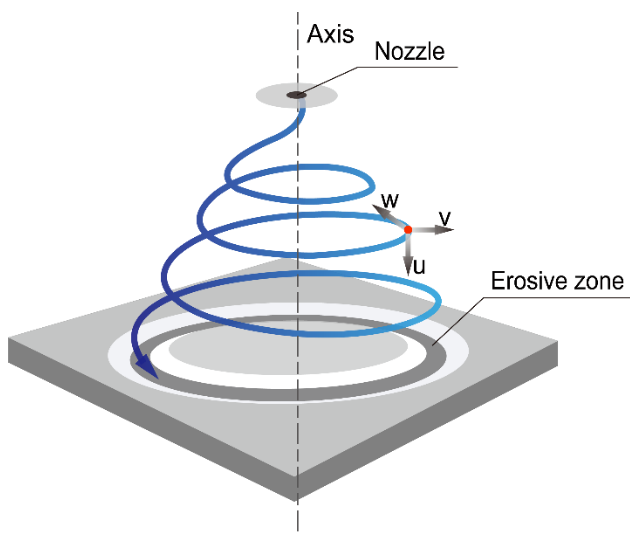

Fig. 6. Rotating water jet principle diagram

The microscopic morphology of the eroded surface of the bamboo powder-HDPE composite at a shooting distance of 0.5 cm and an erosion duration of 180 s are presented in Fig. 7. All eroded surfaces exhibited obvious bamboo fiber crushing and HDPE matrix brittle fracture. There were no nanoscale SiO_2 fillers observed in the eroded surface. This was taken as evidence that nanoscale SiO_2 had been uniformly distributed in the composite system. According to tribology and rotating jet theory, the erosion wear mechanism of bamboo powder-HDPE composites under the action of rotating SCWJ can be divided into three stages in terms of time sequence. The first is the primary damage to the surface plastic layer of the bamboo powder-HDPE composites by the rotating jet under the action of "water hammer" pressure, which were rapidly deprived under the joint action of water jet droplets and garnet sand, and further formed the primary craters on their surfaces (this process was dominated by the garnet sand). Secondly, many micro-pores and micro-cracks were generated around the crater under the tensile and shear breakage caused by the axial and tangential velocities (the most important factor for the damage of composites; among them, tensile failure caused by the axial velocity is the main factor). Finally, the jet pressure was transformed into quasi-static pressure due to the penetration of the rotating jet wedged into the micro-pores and micro-cracks of composites, resulting in "water wedge effect" and making the crack continue to expand under the action of tension. The expanded micro-pores, micro-cracks continued to converge and eventually formed macroscopic damage of composites (Du 2016).

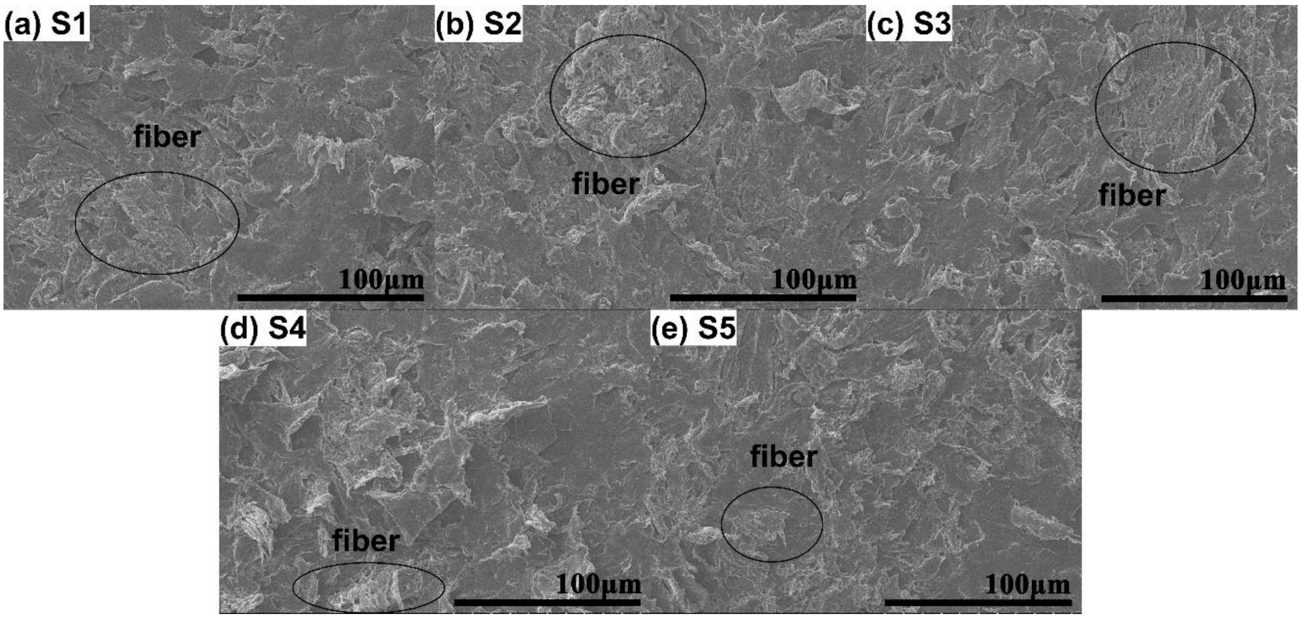

Fig. 7. Microstructure of the eroded surface of bamboo powder-HDPE composite: shooting distance 1.5 cm, duration of erosion 180 s

Elemental Changes and Distribution

Oxygen (O) and silicon (Si) elements are the representative components of bamboo fibers, garnet sand, and silicon dioxide (SiO_2). The test of the elemental distribution and changes of oxygen and silicon in composites before and after erosion could provide important information related to the erosion wear at the chemical composition level. In view of this, the EDS spectra of the bamboo powder-HDPE composites on eroded and uneroded surfaces are given in Fig. 8. All composites showed a tendency of the increasing of oxygen content and the decreasing of the silicon content after undergoing an erosion process. A plausible explanation is that the HDPE matrix of the composites surface layer was degraded by the jet carrying garnet sand and causing the exposure of the bamboo fibers embedded under the HDPE matrix. The bamboo fibers contain more oxygen than the HDPE matrix, and the peeled-off HDPE from the surface layer could increase the overall oxygen content. However, due to the lack of HDPE matrix wrapping, the polar hydroxyl group (-OH) in the bamboo fiber combined with water to form hydrogen bonds could also lead to the increase of oxygen content. In addition, compared with samples S1, S2, S4, and S5, the sample S3 has the lowest oxygen content before and after erosion. As above analysis, S3 has a better fiber/matrix interface, the bamboo fibers were well wrapped by the HDPE matrix, the "anchoring" between two phases was stronger, and the mutual force was greater. Hence, there were less bamboo fibers exposed to the air on the surface of S3 before and after the SCWJ erosion.

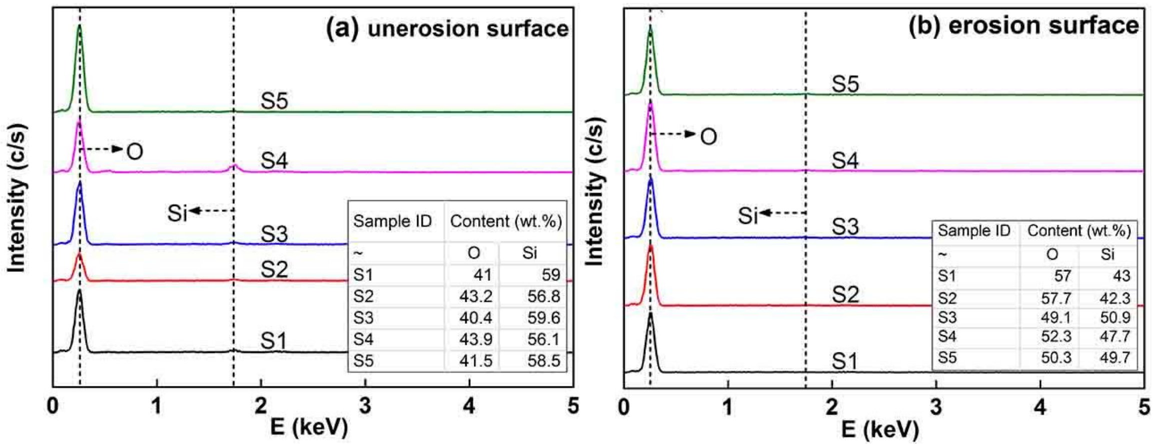

Fig. 8. EDS spectra of the eroded and uneroded surfaces of bamboo powder-HDPE composites

CONCLUSIONS

1. The structural strength and composite structure of the composites can be enhanced by adding nanoscale SiO_2, which is ascribed to the physical cross-linking formed by SiO_2 and macromolecular chain of high-density polyethylene (HDPE). However, the excessive SiO_2 content will in turn reduce their structural strength and composite structure, due to the agglomeration of SiO_2.
2. There is a high correspondence between the erosion wear resistance of composites and their impact strength. In this study, the maximum erosion wear rate was observed at the shooting distance of 0.5 cm and erosion time of 180 s.
3. The scanning electron microscopy (SEM) images and energy-dispersive X-ray spectrometry (EDS) spectra of unworn and worn surfaces revealed various erosive wear mechanisms. These mainly include the pulverization of bamboo fibers, brittle fracture of HDPE matrix, and increase in O content.
4. Using nanoscale SiO_2 as a filler material can enhance the erosion resistance of the composite. Therefore, they can be recommended for use in coastal environments such as trestles, fences, and pontoons.

ACKNOWLEDGMENTS

This research was funded by the Natural Science Foundation of the Higher Education Institutions of Anhui Province (Grant. Nos. KJ2020A0283 and KJ2020A0285) and Agricultural Production Waste Resource Utilization Equipment Innovative Research Group of Science and Technology Innovative Engineering of Chinese Academy of Agricultural Sciences.

REFERENCES CITED

ASTM D256-10 (2018). "Standard test methods for determining the izod pendulum impact resistance of plastics," ASTM International, West Conshohocken, United States.

Asgari, M., Abouelmagd, A., and Sundararaj, U. (2017). "Silane functionalization of sodium montmorillonite nanoclay and its effect on rheological and mechanical properties of HDPE/clay nanocomposites," *Applied Clay Science* 146, 439-448. DOI: 10.1016/j.clay.2017.06.035

Bagci, M., and Imrek, H. (2016). "Erosion wear performance of borax filled novel hybrid composites by using the Taguchi experimental design," *Industrial Lubrication and Tribology* 68(1), 134-140. DOI: 10.1108/ILT-01-2015-0007

Chand, N., Ghosh, A., and Dwivedi, U. K. (2007). "Abrasive wear behaviour of bamboo (*Dendrocalamus strictus*) powder filled polyester composites," *BioResources* 2(4), 693-698. DOI: 10.15376/biores.2.4.693-698

Du, P. (2016). *Study on the Flow Field and Rock Breaking Mechanism of Straight-swirling Integrated Jet*, Master's Thesis, Chongqing University, Chongqing, China.

Fang, Y., Wang, Q., Guo, C., Song, Y., and Cooper, P. A. (2013). "Effect of zinc borate and wood flour on thermal degradation and fire retardancy of polyvinyl chloride (PVC) composites," *Journal of Analytical and Applied Pyrolysis* 100, 230-236. DOI: 10.1016/j.jaap.2012.12.028.

GB/T 1034 (2008). "Plastics – Determination of water absorption," Standardization Administration of China, Beijing, China.

GB/T 2411 (2008). "Plastics and ebonite-Determination of indentation hardness by means of a durometer (shore hardness)," Standardization Administration of China, Beijing, China.

Guo, Y., Li, D., Chen, Y., Liu, S., and Xiong, F. (2014). "Effect of wood flour content on thermo and rheological properties of PE-HD/wood composites," *Engineering Plastics Application* 42(01), 31-35. DOI: 10.3969/j.issn.1001-3539.2014.01.007.

Gupta, A. (2018a). "Synthesis and erosion wear analysis of short bamboo fiber reinforced epoxy composites filled with ceramic fillers," *International Journal of Surface Engineering and Interdisciplinary Materials Science* 6(2), 50-62. DOI: 10.4018/IJSEIMS.2018070104

Gupta, A. (2018b). "Synthesis and erosion wear analysis of short bamboo fiber reinforced epoxy composites filled with ceramic fillers," *International Journal of Surface Engineering and Interdisciplinary Materials Science* 6(2), 50-62. DOI: 10.4018/IJSEIMS.2018070104

Gupta, A., Kumar, A., Patnaik, A., and Biswas, S. (2012). "Effect of filler content and alkalization on mechanical and erosion wear behavior of CBPD filled bamboo fiber composites," *Journal of Surface Engineered Materials and Advanced Technology* 02(03), 149-157. DOI: 10.4236/jsemat.2012.23024

Jeamtrakull, S., Kositchaiyong, A., Markpin, T., Rosarpitak, V., and Sombatsompop, N. (2012). "Effects of wood constituents and content, and glass fiber reinforcement on wear behavior of wood/PVC composites," *Composites Part B: Engineering* 43(7), 2721-2729. DOI: 10.1016/j.compositesb.2012.04.031

Jena, H., Pradhan, A. K., and Pandit, M. K. (2018). "Study of solid particle erosion wear behavior of bamboo fiber reinforced polymer composite with cenosphere filler," *Advances in Polymer Technology* 37(3), 761-769. DOI: 10.1002/adv.21718

Jiang, L., He, C., Fu, J., and Chen, D. (2017). "Wear behavior of wood−plastic composites in alternate simulated sea water and acid rain corrosion conditions," *Polymer Testing* 63, 236-243. DOI: 10.1016/j.polymertesting.2017.08.031
Jiang, L., He, C., Wang, L., and Jiang, C. (2019). "Comparison of seawater corrosion resistance of four types of plant fibers/high-density polyethylene composites," *Acta Materiae Compositae Sinica* 36(07), 1625-1632. DOI: 10.13801/j.cnki.fhclxb.20181023.001
Moreno, D. D. P., Hirayama, D., and Saron, C. (2018). "Accelerated aging of pine wood waste/recycled LDPE composite," *Polymer Degradation and Stability* 149, 39-44. DOI: 10.1016/j.polymdegradstab.2018.01.014
Rashid, B., Leman, Z., Jawaid, M., Ghazali, M. J., Ishak, M. R., and Abdelgnei, M. A. (2017). "Dry sliding wear behavior of untreated and treated sugar palm fiber filled phenolic composites using factorial technique," *Wear* 380-381, 26-35. DOI: 10.1016/j.wear.2017.03.011
Swain, P. T. R., and Biswas, S. (2017). "Abrasive wear behaviour of surface modified jute fiber reinforced epoxy composites," *Materials Research* 20(3), 661-674. DOI: 10.1590/1980-5373-mr-2016-0541
Tewari, U. S., Harsha, A. P., Häger, A. M., and Friedrich, K. (2003). "Solid particle erosion of carbon fibre- and glass fibre-epoxy composites," *Composites science and technology* 63(3), 549-557. DOI: 10.1016/S0266-3538(02)00210-5
Tilly, G. P. (1969). "Erosion caused by airborne particles," *Wear* 14, 63-79. DOI: 10.1016/0043-1648(69)90035-0
Vigneshwaran, S., Uthayakumar, M., and Arumugaprabu, V. (2019). "Solid particle erosion study on redmud - An industrial waste reinforced sisal/polyester hybrid composite," *Materials Research Express* 6(6), 65307. DOI: 10.1088/2053-1591/ab0a44
Wang, L., He, C., and Yang, X. (2019). "Anti-aging and thermal behavior of rice husk/polyvinyl chloride composites by four pretreatment methods," *Acta Materiae Compositae Sinica* 36(11), 2587-2594. DOI: 10.13801/j.cnki.fhclxb.20190326.003
Xue, W. (2016). "Research on application of wood-plastic composites in the city landscape," *Plastics Science and Technology* 44(12), 47-50. DOI: 10.15925/j.cnki.issn1005-3360.2016.12.006
Zhang, Y., Xu, Y., Song, Y., and Zheng, Q. (2013). "Study of poly(vinyl chloride)/acrylonitrile-styrene-acrylate blends for compatibility, toughness, thermal stability and UV irradiation resistance," *Journal of Applied Polymer Science* 130(3), 2143-2151. DOI: 10.1002/app.39405
Zhang, H. (2014). "Effect of a novel coupling agent, alkyl ketene dimer, on the mechanical properties of wood-plastic composites," *Materials & Design* 59, 130-134. DOI: 10.1016/j.matdes.2014.02.048
Zhang, J., Ning, L., Yang, H., Wu, B., Luo, S., and Rong, Z. (2016). "Effects of glass fiber content on properties of bamboo flour/high density polyethylene composites," *Acta Materiae Compositae Sinica* 33(03), 477-485. DOI: 10.13801/j.cnki.fhclxb.20150623.004

Article submitted: April 26, 2022; Peer review completed: July 11, 2022; Revised version received and accepted: July 13, 2022; Published: July 20, 2022.
DOI: 10.15376/biores.17.3.5178-5189